

Mathematic model analysis of Gaussian beam propagation through an arbitrary thickness random phase screen

Yuzhen Tian,^{1,2,3,*} Jin Guo,^{1,2} Rui Wang,^{1,2} and Tingfeng Wang,^{1,2}

¹State Key Laboratory of Laser Interaction with Matter, Changchun 130033, China

²Changchun Institute of Optics, fine Mechanics and Physics, Chinese Academy of Science, Changchun 130033, China

³Graduate University of Chinese Academy of Sciences, Beijing 100039, China

*tyzai@163.com

Abstract: In order to research the statistical properties of Gaussian beam propagation through an arbitrary thickness random phase screen for adaptive optics and laser communication application in the laboratory, we establish mathematic models of statistical quantities, which are based on the Rytov method and the thin phase screen model, involved in the propagation process. And the analytic results are developed for an arbitrary thickness phase screen based on the Kolmogorov power spectrum. The comparison between the arbitrary thickness phase screen and the thin phase screen shows that it is more suitable for our results to describe the generalized case, especially the scintillation index.

©2011 Optical Society of America

OCIS codes: (010.1290) Atmospheric optics; (010.1300) Atmospheric propagation; (010.1330) Atmospheric turbulence; (010.1080) Adaptive optics; (060.4510) Optical communications.

References and links

1. C. Chao, L. Hu, and Q. Mu, "Bandwidth requires of adaptive optical system for horizontal turbulence correction," *Opt. Precision Eng.* **18**(10), 2137–2142 (2010).
2. B. Wang, Z.-y. Wang, and J.-l. Wang, J.-Y. Zhao, Y.-H. Wu, S.-X. Zhang, L. Dong, and M. Wen, "Phase-diverse speckle imaging with two cameras," *Opt. Precision Eng.* **19**(6), 1384–1390 (2011).
3. H. G. Booker, J. A. Ferguson, and H. O. Vats, "Comparison between the extended-medium and the phase-screen scintillation theories," *J. Atmos. Terr. Phys.* **47**(38), 1–399 (1985).
4. L. C. Andrews and R. L. Phillips, *Laser Beam Propagation through Random Media*, 2nd ed. (SPIE, 2005).
5. L. C. Andrews, R. L. Phillips, and A. R. Weeks, "Propagation of a Gaussian-beam wave through a random phase screen," *Waves Random Media* **7**(2), 229–244 (1997).
6. L. C. Andrews, W. B. Miller, and J. C. Ricklin, "Propagation through complex optical system: a phase screen analysis," *SPIE* **2312**, 122–129 (1994).
7. L. C. Andrews and W. B. Miller, "Single- and double-pass propagation through complex paraxial optical systems," *J. Opt. Soc. Am. A* **12**(1), 137–150 (1995).
8. S. V. Mantravadi, T. A. Rhoadarmer, and R. S. Glas, "Simple laboratory system for generating well-controlled atmospheric-like turbulence," *Proc. SPIE* **5553**, 290–300 (2004).
9. X. J. Gan, J. Guo, and Y. Y. Fu, "The simulating turbulence method of laser propagation in the inner field," *J. Phys. Conf. Ser.* **48**, 907–910 (2006).
10. B. D. Zhang, S. Qin, and X. S. Wang, "Accurate and fast simulation of Kolmogorov phase screen by combining spectral method with Zernike polynomials method," *Chin. Opt. Lett.* **8**(10), 969–971 (2010).
11. M. X. Qian, W. Y. Zhu, and R. Rao, "Phase screen distribution for simulating laser propagation along an inhomogeneous atmospheric path," *Acta Phys. Sinica* **58**(9), 6633–6639 (2009).
12. M. Gao and Z. Wu, "Experiments of effect of beam spreading of far-field on aiming deviation," *Opt. Precision Eng.* **18**(3), 602–608 (2010).
13. Y.-h. Gao, Z.-y. An, and N.-n. Li, W.-x. Zhao, and J.-s. Wang, "Optical design of Gaussian beam shaping," *Opt. Precision Eng.* **19**(7), 1464–1471 (2011).
14. V. I. Tatarskii, *Wave Propagation in a Turbulent Medium* (New York: McGraw-Hill, 1961).

1. Introduction

In order to research the statistical properties of Gaussian beam propagation through random media in the laboratory for AO [1,2] and laser communication applications, the random phase screen, which is located between optical source and receiver, is usually used to simulate an extended random medium; therefore it is important to establish the mathematic model of statistical quantities involved in Gaussian beam propagation through a random phase screen. Booker et al. [3] show the mathematic model of a plane wave incident on a phase screen which is centrally located and has the same refractive index spectrum with the extended medium. Andrews et al. [4–7] apply cross-link propagation method to discuss the mathematic model of Gaussian beam propagation through a thin phase screen. Mantravadi [8] and Gan et al. [9] use random phase plates to simulate extended media with different strength, and discuss the relationship between the turbulence strength and the optical system. Many scholars [10,11] utilize numerical method to generate random phase screens, based on which simulate Gaussian beam propagation through atmosphere turbulence.

In this paper, we will, based on the Rytov weak fluctuation method and the thin phase screen model of Andrews et al. [5], research the statistical property of Gaussian beam propagation through an arbitrary thickness phase screen, establish the mathematic models of involving statistical quantities, and develop the analytical results. The application scope of our results will be discussed based on the comparison between the thin phase screen models and arbitrary thickness models.

2. Gaussian beam parameters

We assume the transmitted wave is a lowest-order Gaussian beam wave that, also called TEM₀₀ wave, in the plane of the emitting aperture of the transmitter at $z = 0$, can be expressed as [4,12,13]

$$z = 0: \quad U_0(r, 0) = a_0 \exp\left(-\frac{r}{w_0^2} - \frac{ikr^2}{2F_0}\right) = a_0 \exp\left(-\frac{1}{2}\alpha_0 kr^2\right), \quad (1)$$

where $r = (x^2 + y^2)^{1/2}$, $\alpha_0 = 2/(kW_0^2) + i/F_0$; a_0 is the optical amplitude, F_0 and W_0 denote the phase front radius of curvature and beam radius at which the field amplitude falls to $1/e$ of that on the beam axis, respectively, and k is the optical wave number. The particular cases $F_0 = \infty$, $F_0 > 0$, and $F_0 < 0$ correspond to collimated, convergent, and divergent beam formats, respectively. Based on paraxial theory, the free space optical wave in the receiver plane at $z = L$ is another Gaussian beam described by [4,12]

$$z = L: \quad U_0(r, L) = \frac{a_0}{p(L)} \exp\left[ikL + \left(-\frac{r}{W^2} - \frac{ikr^2}{2F}\right)\right] = \frac{a_0}{p(L)} \exp\left[ikL - \frac{1}{2}\left(\frac{\alpha_0 kr^2}{p(L)}\right)\right], \quad (2)$$

where W and F denote the receiver plane phase front radius of curvature and beam radius, respectively, and $p(L) = 1 + i\alpha_0 L$ is the propagation parameter.

Figure 1 shows the model of Gaussian beam propagation through an arbitrary thickness random phase screen, which the input and output plane are fixed and move the phase screen with thickness $d = L_2$ to modulate the phase of optical field. In the paper, all the three beam case, $F_0 = \infty, F_0 > 0$ and $F_0 < 0$, will be contained, and the beam waist appears in the middle of the optical path. Based on this figure, the nondimensional input plane beam parameters [4–7] are

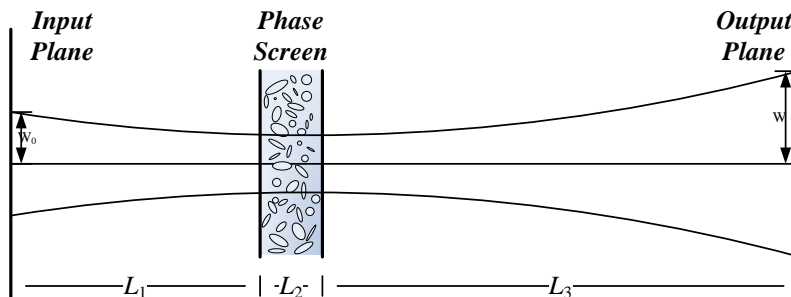


Fig. 1. The model of Gaussian beam propagation through a random phase screen

$$\Theta_0 = 1 - \frac{L}{F_0} \quad \Lambda_0 = \frac{2L}{kW_0^2}. \quad (3)$$

For mathematical simplification, express W and F as

$$W = W_0 \sqrt{\Theta_0^2 + \Lambda_0^2} \quad F = \frac{F_0(\Theta_0^2 + \Lambda_0^2)(\Theta_0 - 1)}{\Theta_0^2 + \Lambda_0^2 - \Theta_0}. \quad (4)$$

As nondimensional input plane beam parameters, introduce the nondimensional parameters of the front plane and posterior plane of the phase screen and the output plan [4–7]

$$z = L_1 \quad \Theta_1 = 1 + \frac{L_1}{F_1} \quad \Lambda_1 = \frac{2L_1}{kW_0^2}, \quad (5)$$

$$z = L_1 + L_2 \quad \Theta_2 = 1 + \frac{L_2}{F_2} \quad \Lambda_2 = \frac{2L_2}{kW_0^2}, \quad (6)$$

$$z = L_1 + L_2 + L_3 \quad \Theta_3 = 1 + \frac{L_3}{F_3} \quad \Lambda_3 = \frac{2L_3}{kW_0^2}. \quad (7)$$

We can calculate the receiver plane propagation parameter $p(L)$, according to Eqs. (5) to (7),

$$\frac{1}{p(L)} = \Theta - i\Lambda = \prod_{i=1}^3 (\Theta_i - i\Lambda_i). \quad (8)$$

3. Rytov method

For the model of Gaussian beam propagation through a random phase screen, showed in Fig. 1, a single phase screen usually can represent weak fluctuation conditions, therefore, the statistical property will be discussed based on Rytov weak fluctuation method [4,14]. In the weak fluctuation condition, propagation path L , the optical field can be expressed as:

$$U(r, L) = U_0(r, L) \exp[\Psi(r, L)] = U_0(r, L) \exp[\psi_1(r, L) + \psi_2(r, L) + \dots], \quad (9)$$

where $U_0(r, L)$ is the free space Gaussian beam, described in Eqs. (2), $\Psi(r, L)$ is a complex phase perturbation due to turbulence, and $\psi_1(r, L)$ and $\psi_2(r, L)$ are the first-order and second-order complex phase perturbations, respectively. It is known that the first two order complex phase perturbations can nearly determinate all the long time statistical property, so we just consider

$\psi_1(r,L)$ and $\psi_2(r,L)$ in this paper. For the case of homogeneous and isotropic extended turbulence, it has been shown by Andrews and Miller [6,7] that all statistical quantities of interest for an optical wave in the weak fluctuation regime are based on linear combinations of the following three second-order moments:

$$E_1(0,0) = \langle \psi_2(\bar{r},L) + \frac{1}{2}\psi_1^2(\bar{r},L) \rangle = -2\pi^2 k^2 \int_0^L dz \int_0^\infty \kappa \Phi_n(\kappa, z) dk, \quad (10)$$

$$\begin{aligned} E_2(\bar{r}_1, \bar{r}_2) &= \langle \psi_1(\bar{r}_1, L) \psi_1^*(\bar{r}_2, L) \rangle \\ &= 4\pi^2 k^2 \int_0^L dz \int_0^\infty d\kappa \kappa \Phi_n(\kappa, z) \exp\left[-\frac{\Lambda \kappa^2 (1-z/L)^2}{k}\right] \\ &\quad \times J_0\left\{\kappa\left[1 - \bar{\Theta}(1-z/L)\right] \rho - 2i\Lambda(1-z/L)r\right\}, \end{aligned} \quad (11)$$

$$\begin{aligned} E_3(\bar{r}_1, \bar{r}_2) &= \langle \psi_1(\bar{r}_1, L) \psi_1(\bar{r}_2, L) \rangle \\ &= -4\pi^2 k^2 \int_0^L dz \int_0^\infty d\kappa \kappa \Phi_n(\kappa, z) \exp\left\{-\frac{ik^2 \gamma L}{k}(1-z/L)\left[1 - \bar{\Theta}(1-z/L)\right]\right\} \\ &\quad \times \exp\left[-\frac{\Lambda \kappa^2 (1-z/L)^2}{k}\right] J_0\left\{\kappa \rho \left[1 - (\bar{\Theta} + i\Lambda)(1-z/L)\right]\right\}, \end{aligned} \quad (12)$$

where $\mathbf{r} = (\mathbf{r}_1 + \mathbf{r}_2)/2$, $\mathbf{p} = \mathbf{r}_1 - \mathbf{r}_2$, $r = |\mathbf{r}|$, $\rho = |\mathbf{p}|$, κ is the space wave number, $\bar{\Theta} = 1 - \Theta$, $J_0(x)$ is the Bessel function of the first kind, the brackets $\langle \rangle$ denote an ensemble average, and the asterisk * denotes the complex conjugate field.

3.1 Arbitrary thickness phase screen

As shown in Fig. 1, the Gaussian beam propagates through an arbitrary thickness phase screen, with thickness $d = L_2$, thus we can assume that random media exist only in $[L_1, L_1 + L_2]$ and change the integral variable:

$$1 - z/L = \xi \quad (0 \leq z \leq L, L_1/L \leq \xi \leq (L_1 + L_2)/L). \quad (13)$$

In this paper, our analysis is based on Kolmogorov spectrum,

$$\Phi_n(\kappa) = 0.033 C_n^2 \kappa^{-11/3}, \quad (14)$$

where the refractive-index structure parameter C_n^2 is assumed constant, because the random media only exist over $L_1 \leq z \leq L_1 + L_2$, so we can set $\Phi_n(\kappa)$ as:

$$\Phi_n(\kappa) = \begin{cases} 0.033 \hat{C}_n^2 \kappa^{-11/3} & L_1 \leq z \leq L_1 + L_2, \\ 0 & \text{others} \end{cases}, \quad (15)$$

where \hat{C}_n^2 denotes the structure constant of the random phase screen, ^ is the corresponding phase screen statistical quantities. Based on these hypothesis and Eqs. (10), (11) and (12), we can obtain the second-order moments of the arbitrary thickness phase screen:

$$\hat{E}_1(0,0) = \langle \psi_2(\bar{r}, L) + \frac{1}{2}\psi_1^2(\bar{r}, L) \rangle = -2\pi^2 k^2 L \int_{\frac{L_2}{L}}^{\frac{L_2+L_3}{L}} d\xi \int_0^\infty \kappa \Phi_n(\kappa) d\kappa, \quad (16)$$

$$\begin{aligned} \hat{E}_2(\bar{r}_1, \bar{r}_2) &= \langle \psi_1(\bar{r}_1, L) \psi_1^*(\bar{r}_2, L) \rangle \\ &= 4\pi^2 k^2 L \int_{\frac{L_2}{L}}^{\frac{L_2+L_3}{L}} d\xi \int_0^\infty d\kappa \kappa \Phi_n(\kappa) \exp\left[-\frac{\Lambda L \kappa^2 \xi^2}{k}\right] \\ &\quad \times J_0\left\{\kappa \left[1 - \bar{\Theta} \xi\right] p - 2i\Lambda \xi r\right\}, \end{aligned} \quad (17)$$

$$\begin{aligned} \hat{E}_3(\bar{r}_1, \bar{r}_2) &= \langle \psi_1(\bar{r}_1, L) \psi_1^*(\bar{r}_2, L) \rangle \\ &= -4\pi^2 k^2 L \int_{\frac{L_2}{L}}^{\frac{L_2+L_3}{L}} d\xi \int_0^\infty d\kappa \kappa \Phi_n(\kappa) \exp\left\{-\frac{i\kappa^2 \gamma L}{k} \xi \left[1 - \bar{\Theta} \xi\right]\right\} \\ &\quad \times \exp\left[-\frac{\Lambda L \kappa^2 \xi^2}{k}\right] J_0\left\{\kappa \rho \left[1 - (\bar{\Theta} + i\Lambda) \xi\right]\right\}, \end{aligned} \quad (18)$$

The three second-order moments are very important for the statistical property of the arbitrary thickness model, for example the mutual coherent function and scintillation index are both the linear combination of the three moments.

3.2 Rytov Variance of Phase Screen

For comparison, introduce Rytov variation of phase screen as Rytov variance in atmosphere. The Rytov variance [15] defines as, for extend random media on whole optical path,

$$\begin{aligned} \sigma_R^2 &= 8\pi^2 k^2 \int_0^L dz \int_0^\infty d\kappa \kappa \Phi_n(\kappa) \left[1 - \cos\left(\frac{\kappa^2(L-z)}{k}\right)\right] \\ &= 1.23 C_n^2 k^{\frac{7}{6}} L^{1\frac{1}{6}}. \end{aligned} \quad (19)$$

Changing the integral variable and interval, we can get the Rytov variance for the arbitrary thickness model:

$$\hat{\sigma}_R^2 = 8\pi^2 k^2 L \int_{\frac{L_2}{L}}^{\frac{L_2+L_3}{L}} d\xi \int_0^\infty d\kappa \kappa \Phi_n(\kappa) \left[1 - \cos\left(\frac{\kappa^2 L \xi}{k}\right)\right]. \quad (20)$$

It is clear that the integral in Eq. (20) does not converge for Kolmogorov spectrum, but we can utilize von Kármán spectrum to deduce approximate result, because note that von Kármán spectrum,

$$\Phi_n(\kappa) = 0.033 C_n^2 \frac{\exp(-\kappa^2/\kappa_m^2)}{(\kappa^2 + \kappa_0^2)^{1/6}}, \quad (21)$$

approximates to Kolmogorov spectrum, when $\kappa_0 \rightarrow 0^+$, $\kappa_m \rightarrow \infty$, and $\kappa_0/\kappa_m \rightarrow 0^+$. Based on von Kármán spectrum and using the integral definition of confluent hypergeometric function and asymptotic formula [4],

$$U(a; c; x) = \frac{1}{\Gamma(a)} \int_0^\infty \exp(-xt) t^{a-1} (1+t)^{c-a-1} dt \quad (a > 0, \text{Re}(x) > 0), \quad (22)$$

$$U(a; c; x) \cong \frac{\Gamma(1-c)}{\Gamma(1+a-c)} + \frac{\Gamma(c-1)}{\Gamma(a)} x^{1-c} \quad (|x| \ll 1), \quad (23)$$

and set $\kappa_0 \rightarrow 0^+$, $\kappa_m \rightarrow \infty$, and $\kappa_0/\kappa_m \rightarrow 0^+$, then we can calculate the integral (20):

$$\begin{aligned}\hat{\sigma}_R^2 &\cong 4.7466 C_n^2 k^{7/6} L^{1/6} \operatorname{Re} \left\{ i^{5/6} \int_{L_3/L}^{(L_2+L_3)/L} \xi^{5/6} d\xi \right\} \\ &= 1.23 C_n^2 k^{7/6} L^{1/6} \left[\left(\frac{L_2+L_3}{L} \right)^{1/6} - \left(\frac{L_3}{L} \right)^{1/6} \right],\end{aligned}\quad (24)$$

where \cong denotes the approximate method. By enforcing the equivalence [5] of Eqs. (19) and (24), one is led to the relation between structure constants

$$C_n^2 = \hat{C}_n^2 \left[\left(\frac{L_2+L_3}{L} \right)^{1/6} - \left(\frac{L_3}{L} \right)^{1/6} \right]. \quad (25)$$

Equations (25) shows that using a phase screen to simulate turbulence depends on the thickness of the phase screen and distance from the phase screen to receiver. It is not practical for doing this comparison, however, the phase screen always used indoors, which the simulation propagation path is shorter than atmosphere propagation path. For the model in Fig. 1, the comparison should be implemented as

$$C_n^2 L_A^{1/6} = \hat{C}_n^2 L^{1/6} \left[\left(\frac{L_2+L_3}{L} \right)^{1/6} - \left(\frac{L_3}{L} \right)^{1/6} \right], \quad (26)$$

where L_A is the propagation path in atmosphere, and L is that in the phase screen model. The left side of Eq. (26) represents the turbulence effects, which are turbulence strength and propagation path, on optical field, and the right side of Eq. (26) represents simulation effects of the phase screen.

4. Mutual coherent function

The second order moment of optical field on receiver plane, known as mutual coherent function (MCF), is defined as in a weak fluctuation condition,

$$\begin{aligned}\Gamma_2(\mathbf{r}_1, \mathbf{r}_2, L) &= \langle U(\mathbf{r}_1, L) U^*(\mathbf{r}_2, L) \rangle \\ &= U_0(\mathbf{r}_1, L) U_0^*(\mathbf{r}_2, L) \exp[2E_1(0,0) + E_2(\mathbf{r}_1, \mathbf{r}_2)] \\ &= \Gamma_2^0(\mathbf{r}_1, \mathbf{r}_2, L) \exp[2E_1(0,0) + E_2(\mathbf{r}_1, \mathbf{r}_2)],\end{aligned}\quad (27)$$

where $\Gamma_2^0(\mathbf{r}_1, \mathbf{r}_2, L)$ is the MCF in free space

$$\Gamma_2^0(\mathbf{r}_1, \mathbf{r}_2, L) = U_0(\mathbf{r}_1, L) U_0^*(\mathbf{r}_2, L) = \frac{W_0^2}{W} \exp\left(-\frac{2r^2}{W^2} - \frac{\rho^2}{2W^2} - i \frac{k}{F} \mathbf{p} \cdot \mathbf{r}\right), \quad (28)$$

Normally we don't calculate $2E_1(0,0) + E_2(\mathbf{r}_1 + \mathbf{r}_2)$ directly, but make some simplification

$$\begin{aligned}\Gamma_2(\mathbf{r}_1, \mathbf{r}_2, L) &= \Gamma_2^0(\mathbf{r}_1, \mathbf{r}_2, L) \exp[2E_1(0,0) + E_2(\mathbf{r}_1, \mathbf{r}_2)] \\ &= \Gamma_2^0(\mathbf{r}_1, \mathbf{r}_2, L) \exp\left[\sigma_r^2(\mathbf{r}_1, L) + \sigma_r^2(\mathbf{r}_2, L) - T - \frac{1}{2} \Delta(\mathbf{r}_1, \mathbf{r}_2, L)\right].\end{aligned}\quad (29)$$

The definitions of variables in right side of Eq. (29) are discussed in [4], and, for a phase screen with thickness $d = L_2$, they are defined as

$$\begin{aligned}\hat{\sigma}_r^2(r, L) &= \frac{1}{2}[E_2(r, r) - E_2(0, 0)] \\ &= 2\pi^2 k^2 L \int_{\frac{L_3}{L}}^{\frac{L_2+L_3}{L}} d\xi \int_0^\infty d\kappa \kappa \Phi_n(\kappa) \exp\left[-\frac{\Lambda L \xi^2 \kappa^2}{k}\right] [I_0(2\Lambda r \xi \kappa) - 1],\end{aligned}\quad (30)$$

$$\begin{aligned}\hat{T} &= -2E_1(0, 0) - E_2(0, 0) \\ &= 4\pi^2 k^2 L \int_{\frac{L_3}{L}}^{\frac{L_2+L_3}{L}} d\xi \int_0^\infty d\kappa \kappa \Phi_n(\kappa) \left[1 - \exp\left(-\frac{\Lambda L \xi^2 \kappa^2}{k}\right)\right],\end{aligned}\quad (31)$$

$$\begin{aligned}\hat{\Delta}(r_1, r_2, L) &= E_2(r_1, r_1) + E_2(r_2, r_2) - 2E_2(r_1, r_2) \\ &= 4\pi^2 k^2 L \int_{\frac{L_3}{L}}^{\frac{L_2+L_3}{L}} d\xi \int_0^\infty d\kappa \kappa \Phi_n(\kappa) \exp\left(-\frac{\Lambda L \xi^2 \kappa^2}{k}\right) \\ &\quad \times \left\{ I_0(2\Lambda r_1 \xi \kappa) + I_0(2\Lambda r_2 \xi \kappa) - 2J_0\left[\left(1 - \bar{\Theta} \xi\right) p - 2i\Lambda \xi r \middle| \kappa \right] \right\},\end{aligned}\quad (32)$$

where $I_0(x) = J_0(ix)$ is the modified Bessel function of the first kind.

4.1 Mean irradiance

For identical observation points, $\mathbf{r}_1 = \mathbf{r}_2 = \mathbf{r}$, the MCF determines the mean irradiance

$$\langle \hat{I}(r, L) \rangle = \Gamma_2(r, r, L) = \frac{W_0^2}{w} \exp\left(-\frac{2r^2}{w^2}\right) \exp\left[2\hat{\sigma}_r^2(r, L) - \hat{T}\right].\quad (33)$$

Using integral Eqs. (30) and (31) can calculate the mean irradiance. Based on the definition of Bessel function, $I_0(x)$, and the property of Gamma function, $\Gamma(x)$,

$$\begin{aligned}I_0(x) &= \sum_{n=0}^{\infty} \frac{(x/2)^{2n}}{n! \Gamma(n+1)} \\ \int_0^\infty e^{-st} t^{x-1} dt &= \frac{\Gamma(x)}{s^x} \quad [\operatorname{Re}(x) > 0, \operatorname{Re}(s) > 0],\end{aligned}\quad (34)$$

we can obtain $\hat{\sigma}_r^2(r, L)$

$$\hat{\sigma}_r^2(r, L) = 0.815 \hat{C}_n^2 k^{7/6} L^{1/6} \Lambda^{5/6} \left[\left(\frac{L_2+L_3}{L}\right)^{8/3} - \left(\frac{L_3}{L}\right)^{8/3} \right] \left[1 - {}_1F_1\left(-\frac{5}{6}; 1; \frac{2r^2}{w^2}\right) \right],\quad (35)$$

where ${}_1F_1(a; c; x)$ is the confluent hypergeometric function.

For the integral in Eq. (31), it is not converge for Kolmogorov spectrum, but we can utilize von Kármán spectrum to approximate as the calculation of $\hat{\sigma}_R^2$ in Eq. (20),

$$\hat{T} \cong 1.63 \hat{C}_n^2 k^{7/6} L^{1/6} \Lambda^{5/6} \left[\left(\frac{L_2+L_3}{L}\right)^{8/3} - \left(\frac{L_3}{L}\right)^{8/3} \right].\quad (36)$$

Thus the mean irradiance for the arbitrary thickness model is

$$\langle I(r, L) \rangle = \frac{w_0^2}{w^2} \exp\left(-\frac{2r^2}{w^2}\right) \exp\left[-1.63 C_n^2 k^{7/6} L^{1/6} \Lambda^{5/6} \left[\left(\frac{L_3+L_2}{L}\right)^{5/3} - \left(\frac{L_3}{L}\right)^{5/3}\right] {}_1F_1\left(-5/6; 1; \frac{2r^2}{w^2}\right)\right]. \quad (37)$$

For the thin phase screen model, the mean irradiance is given in [5]

$$\langle I(r, L) \rangle = \frac{w_0^2}{w^2} \exp\left(-\frac{2r^2}{w^2}\right) \exp\left[-1.93 \hat{\sigma}_R'^2 (\Lambda d_3)^{5/6} {}_1F_1\left(-5/6; 1; \frac{2r^2}{w^2}\right)\right], \quad (38)$$

where

$$\hat{\sigma}_R'^2 = 2.25 \hat{C}_n^2 k^{7/6} L_2 L_3^{5/6} \quad (39)$$

is the Rytov variance for thin phase screen, and $d_3 = L_3/L$.

In order to compare the two model, as shown in Fig. 1, the Gaussian beam propagates through a random phase screen with different thickness and propagation path $L = 1\text{m}$, and move the phase screen between transmitter and receiver to change the receive plane optical field. Figure 2 gives the comparison of the mean irradiance for two models, as a function of $(k\rho^2/L)^{1/2}$. We can find out that there are few differences between Eqs. (37) and (38), even for thick phases ($d/L = 0.1, d = 100\text{mm}$), so the thin phase screen model for the mean irradiance can approximate to the arbitrary model well.

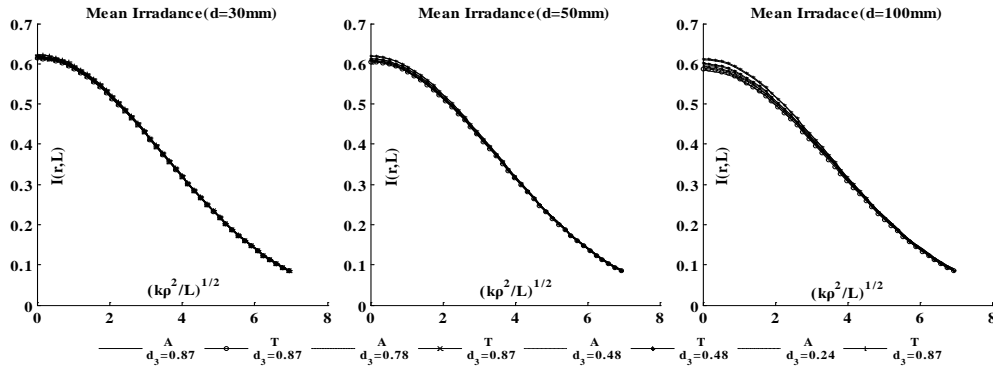


Fig. 2. Comparison between mean irradiance of thin phase screen and that of arbitrary thickness (T: thin phase screen; A: arbitrary thickness phase screen; $d_3 = L_3/L$)

4.2 Mutual coherent function

Because the MCF of Gaussian beam propagation through an arbitrary thickness phase screen depends on the position of the two observation points, it is statistically inhomogeneous. However, it is a function of only the distant of the two points ρ , when they are central symmetry about optical axis, $\mathbf{r}_1 = -\mathbf{r}_2$,

$$\hat{\Gamma}_2(\rho, L) = \frac{w_0^2}{w^2} \exp\left(-\frac{1}{4} \frac{\Lambda k \rho^2}{L}\right) \exp\left[-\hat{T} - \frac{1}{2} \hat{d}(\rho, L)\right], \quad (40)$$

where

$$\hat{d}(\rho, L) = 8\pi^2 k^2 L \int_{\frac{L_3}{L}}^{\frac{L_2+L_3}{L}} d\xi \int_0^\infty d\kappa \kappa \Phi_n(\kappa) \exp\left(-\frac{\Lambda \kappa^2 \xi^2}{k}\right) \left\{1 - J_0\left[(1 - \bar{\Theta}\xi)\kappa\rho\right]\right\}. \quad (41)$$

It is hard to develop the analytic result for integral (41), but we can simplify it for numerical calculation. Use the series representation of Bessel function and confluent hypergeometric function

$$J_0(x) = \sum_{n=0}^{\infty} \frac{(-1)^n (x/2)^{2n}}{n! \Gamma(n+1)} \quad {}_1F_1(a; c; x) = \sum_{n=0}^{\infty} \frac{(a)_n x^n}{(c)_n n!} \quad (42)$$

to deduce Eq. (41),

$$\hat{d}(\rho, L) = 8.70 \hat{C}_n^2 k^{7/6} L^{1/6} \Lambda^{5/6} H, \quad (43)$$

where

$$H = \int_{\frac{L_2}{L}}^{\frac{L_2+L_3}{L}} \xi^{5/3} \left\{ {}_1F_1 \left[-5/6; 1; -\frac{(1-\bar{\Theta}\xi)^2 k \rho^2}{4\Lambda L \xi^2} \right] - 1 \right\} d\xi. \quad (44)$$

According to these results, it is easy to get the normalized MCF

$$\frac{\hat{\Gamma}_2(\rho, L)}{\hat{\Gamma}_2(0, L)} = \exp \left[-\frac{1}{4} \frac{\Lambda k \rho^2}{L} - \frac{1}{2} \hat{d}(\rho, L) \right], \quad (45)$$

where $\hat{\Gamma}_2(0, L)$ is on axis value of the MCF. [5] gives the normalized MCF for thin phase screen model:

$$\frac{\hat{\Gamma}'_2(\rho, L)}{\hat{\Gamma}'_2(0, L)} = \exp \left[-\frac{1}{4} \frac{\Lambda k \rho^2}{L} - 1.179 \hat{\sigma}_R'^2 \left| 1 - \bar{\Theta} d_3 \right|^{5/3} \left(\frac{k \rho^2}{L} \right)^{5/6} \right], \quad (46)$$

Figure 3 plots the comparison of MCF, which is shown as a function of $(k\rho^2/L)^{1/2}$, for arbitrary thickness model and thin phase screen model. From the comparison in Fig. 3, the difference of MCF for two models, Eqs. (45) and (46), is not apparent when the phase screen relative thickness d/L is less than 0.01 ($d = 10mm$), but it increase as the thickness increasing. The MCF for thin phase screen approximation is more accurate when the phase screen is near to the receiver plane than it is in other position. Therefore, it is better to use Eq. (45), MCF for arbitrary thickness model, to describe the normalized MCF when the relative thickness d/L is greater than 0.01. As a whole tendency, the MCF decreases as the separation distance ρ of two observation points increasing, which means that the further the two observation points separate, the worse the relativity of the two observation points is. And the weakening of the relativity of the two points is more severe when the phase screen is close to input plane.

4.3 Modulus of the complex degree of coherent

In addition to obtain the mean irradiance, the MCF can also be used to calculate the loss of spatial coherence of an initially coherent beam, which can be deduced form the modulus of the complex degree of coherence (DOC) [4]

$$\begin{aligned} \text{DOC}(r_1, r_2, L) &= \frac{|\Gamma_2(r_1, r_2, L)|}{\sqrt{\Gamma_2(r_1, r_1, L) \Gamma_2(r_2, r_2, L)}} \\ &= \exp \left[-\frac{1}{2} D(r_1, r_2, L) \right], \end{aligned} \quad (47)$$

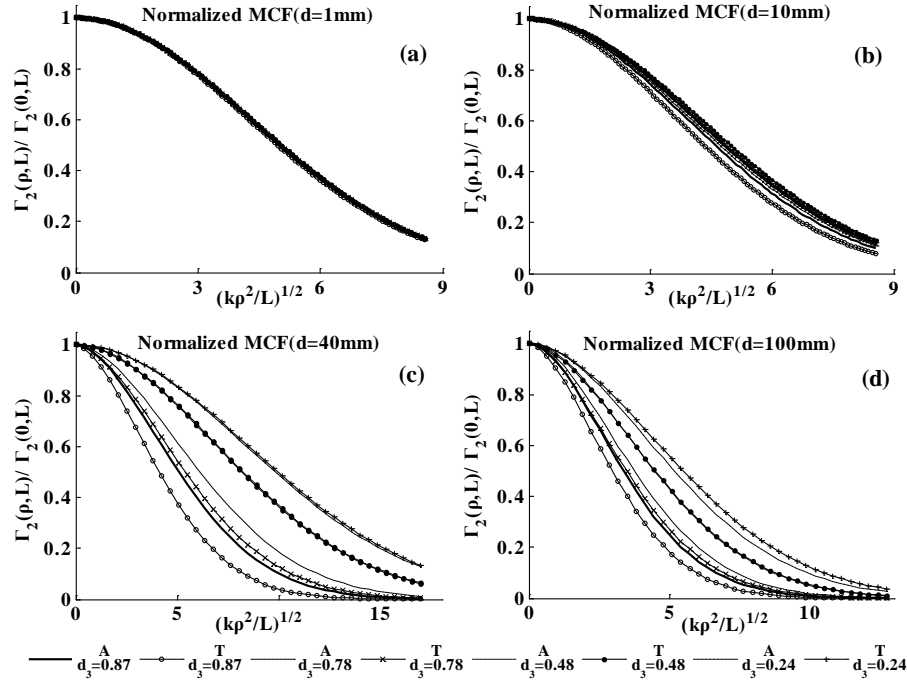


Fig. 3. Comparison between normalized MCF of thin phase screen and that of arbitrary thickness (T: thin phase screen; A: arbitrary thickness phase screen; $d_3 = L_3/L$)

where $D(\mathbf{r}_1, \mathbf{r}_2, L) = \text{Re}[\Delta(\mathbf{r}_1, \mathbf{r}_2, L)]$ is the wave structure function (WSF). Written as a function of separation distance ρ , $\text{DOC}(\rho, r, L)$ and $D(\rho, r, L)$, the spatial coherence radius ρ_0 is defined by $\text{DOC}(\rho_0, r, L) = 1/e$ or $D(\rho_0, r, L) = 2$.

For central symmetry observation points, $\mathbf{r}_1 = -\mathbf{r}_2$, the WSF for Gaussian beam propagation through an arbitrary thickness phase screen can be expressed as

$$\hat{D}(\rho, L) = 8\pi^2 k^2 L \int_{\frac{L_2}{L}}^{\frac{L_2+L_3}{L}} d\xi \int_0^\infty d\kappa \kappa \Phi_n(\kappa) \exp\left(-\frac{\Lambda \kappa^2 \xi^2}{k}\right) \left\{ I_0(\Lambda \rho \xi \kappa) - J_0\left[(1 - \bar{\Theta} \xi) \kappa \rho\right] \right\} \quad (48)$$

$$= \hat{d}(\rho, L) + 4\hat{\sigma}_r^2(\rho/2, L).$$

For thin phase screen approximation, the WSF [5] is

$$\hat{D}'(\rho, L) = 7.074 \hat{\sigma}_R^2 \left(\Lambda d_3^2 \right)^{5/6} \left\{ {}_1F_1\left[-5/6; 1; -\frac{(1-\bar{\Theta}d_3)^2 k \rho^2}{4\Lambda L d_3^2}\right] - {}_1F_1\left[-5/6; 1; \frac{k\Lambda \rho^2}{4L}\right] \right\}. \quad (49)$$

Based on Eqs. (48) and (49), we can calculate the DOC by the two methods. Figure 4 plots the DOC, as a function of $2L_1/kW_0^2$, for different thickness phase screen. The DOC, deduced by thin phase screen approximation, can only approximate the spatial coherent loss when the phase screen is located near the beam waist, and the further away from beam waist the phase screen is, the greater the differences between the two models, Eqs. (48) and (49), are. For the arbitrary thickness model, the DOC is near unit when the phase screen is close to beam waist, and it gets down as the phase screen is far away from beam waist. So the DOC [5] for thin phase screen is suitable for describing the beam waist coherence, but for describing the coherence of other position, we should use the DOC for arbitrary thickness model.

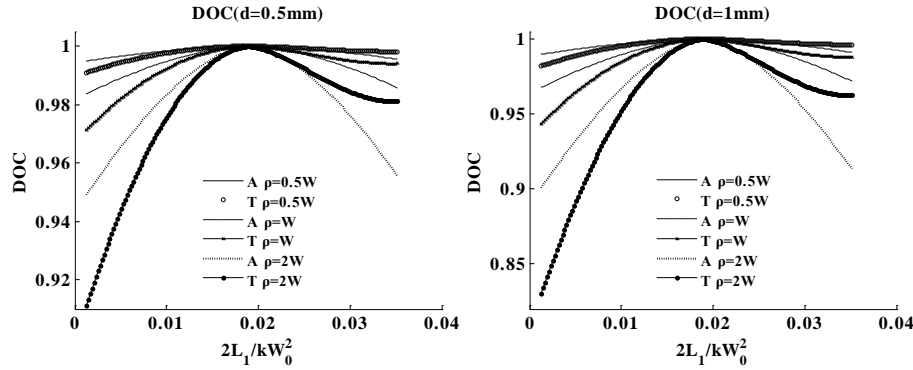


Fig. 4. Comparison the DOC of thin and arbitrary thickness phase screen (T: thin phase screen; A: arbitrary thickness phase screen)

5. Scintillation index

Scintillation index $\sigma_I^2(\mathbf{r}, L)$, one of the most important components of fourth order field moment, describes the irradiance fluctuation on receiver plane. When the log-amplitude variance is sufficiently small $\sigma_\chi^2 = 1$, which is usually valid, the scintillation index [4] is defined as

$$\sigma_I^2(\mathbf{r}, L) = \exp[4\sigma_\chi^2(\mathbf{r}, L)] - 1 \cong 4\sigma_\chi^2(\mathbf{r}, L) = 2 \operatorname{Re}[E_2(\mathbf{r}, \mathbf{r}) + E_3(\mathbf{r}, \mathbf{r})]. \quad (50)$$

For mathematic simplification, it is convenient to express the scintillation index as a sum of radial and longitudinal components, $\sigma_{I,r}^2(\mathbf{r}, L)$ and $\sigma_{I,l}^2(L)$, in the form [4]

$$\sigma_I^2(\mathbf{r}, L) = \sigma_{I,r}^2(\mathbf{r}, L) + \sigma_{I,l}^2(L) = 4\sigma_r^2(\mathbf{r}, L) + \sigma_{I,l}^2(L). \quad (51)$$

For phase screen case, $\hat{\sigma}_r^2(\mathbf{r}, L)$ has been given by Eq. (35). $\hat{\sigma}_{I,l}^2(L)$, the longitudinal component, is defined as

$$\hat{\sigma}_{I,l}^2(L) = 8\pi^2 k^2 L \int_{\frac{L_2}{L}}^{\frac{L_2+L_3}{L}} d\xi \int_0^\infty d\kappa \kappa \Phi_n(\kappa) \exp[-\frac{N\xi^2}{k} \kappa^2] \{1 - \cos[\frac{L\kappa^2}{k} \xi(1 - \bar{\Theta}\xi)]\}. \quad (52)$$

Based on the property of the Gamma function $\Gamma(x)$ [15]

$$\int_0^\infty x^{\lambda-1} (e^{-\mu x} - e^{-\nu x}) dx = \Gamma(\lambda) (\mu^{-\lambda} - \nu^{-\lambda}) \quad \operatorname{Re}(\lambda) > 2, \operatorname{Re}(\mu) > 0, \operatorname{Re}(\nu) > 0, \quad (53)$$

and the integral equation [4]

$$\int_0^x \frac{t^{\mu-1}}{(1+\beta t)^\nu} dt = \frac{x^\mu}{\mu} {}_2F_1(\nu, \mu; 1+\mu; -\beta x) \quad \operatorname{Re}(\mu) > 0, \quad (54)$$

we can deduce the longitudinal component $\hat{\sigma}_{I,l}^2(L)$

$$\hat{\sigma}_{I,l}^2(L) = 4.74\hat{C}_n^2 k^{\frac{7}{6}} L^{\frac{11}{6}} \operatorname{Re} \left\{ i^{\frac{5}{6}} \left(\frac{L_3+L_2}{L} \right)^{11/6} {}_2F_1 \left[-\frac{5}{6}, \frac{11}{6}; \frac{17}{6}; (\bar{\Theta} + i\Lambda) \frac{L_3+L_2}{L} \right] \right. \\ \left. - i^{\frac{5}{6}} \left(\frac{L_3}{L} \right)^{11/6} {}_2F_1 \left[-\frac{5}{6}, \frac{11}{6}; \frac{17}{6}; (\bar{\Theta} + i\Lambda) \frac{L_3}{L} \right] - \frac{11}{16} \Lambda^{\frac{5}{6}} \left[\left(\frac{L_3+L_2}{L} \right)^{8/3} - \left(\frac{L_3}{L} \right)^{8/3} \right] \right\}. \quad (55)$$

So the scintillation index for Gaussian beam propagation through an arbitrary thickness phase screen is the sum of Eqs. (35) and (55)

$$\hat{\sigma}_I^2(r, L) = 4\hat{\sigma}_r^2(r, L) + \hat{\sigma}_{I,l}^2(L) \\ = 3.26\hat{C}_n^2 k^{\frac{7}{6}} L^{\frac{11}{6}} \Lambda^{\frac{5}{6}} \left[\left(\frac{L_3+L_2}{L} \right)^{\frac{8}{3}} - \left(\frac{L_3}{L} \right)^{\frac{8}{3}} \right] \left[1 - {}_1F_1 \left(-\frac{5}{6}; 1; \frac{2r^2}{W^2} \right) \right] \\ + 4.74\hat{C}_n^2 k^{\frac{7}{6}} L^{\frac{11}{6}} \operatorname{Re} \left\{ i^{\frac{5}{6}} \left(\frac{L_3+L_2}{L} \right)^{11/6} {}_2F_1 \left[-\frac{5}{6}, \frac{11}{6}; \frac{17}{6}; (\bar{\Theta} + i\Lambda) \frac{L_3+L_2}{L} \right] \right. \\ \left. - i^{\frac{5}{6}} \left(\frac{L_3}{L} \right)^{11/6} {}_2F_1 \left[-\frac{5}{6}, \frac{11}{6}; \frac{17}{6}; (\bar{\Theta} + i\Lambda) \frac{L_3}{L} \right] - \frac{11}{16} \Lambda^{\frac{5}{6}} \left[\left(\frac{L_3+L_2}{L} \right)^{8/3} - \left(\frac{L_3}{L} \right)^{8/3} \right] \right\}. \quad (56) \\ (r \leq W)$$

Taking the thin phase screen approximation, the scintillation index is given in [5]

$$\hat{\sigma}_I^2(r, L) = 6.45\hat{\sigma}_R^2 (\Lambda d_3)^{\frac{5}{6}} \left(\frac{r^2}{W^2} \right) \\ + 3.87\hat{\sigma}_R^2 \left\{ \left[(\Lambda d_3)^2 + (1 - \bar{\Theta} d_3)^2 \right]^{\frac{1}{2}} \cos \left[\frac{5}{6} \arctan \left(\frac{1 - \bar{\Theta} d_3}{\Lambda d_3} \right) \right] - (\Lambda d_3)^{\frac{5}{6}} \right\}. \quad (57) \\ (r \leq W)$$

Figure 4 plots the scintillation index, for Gaussian beam propagation through different thickness phase screens, which relative thickness d/L are 10^{-4} and 0.01, as a function of the phase screen position $2L_1/kW_0^2$. From Fig. 4, it is clear that there are apparent differences between the two models, Eqs. (56) and (57), even for the thin phase screen, $d/L = 10^{-4}$. For the relationship described by Eq. (56), the scintillation index is get down firstly and then increasing, as the phase screen moving from input plane to output plane, and it obtain the minimum value when the phase screen is located in beam waist. The scintillation index is in direct proportion to

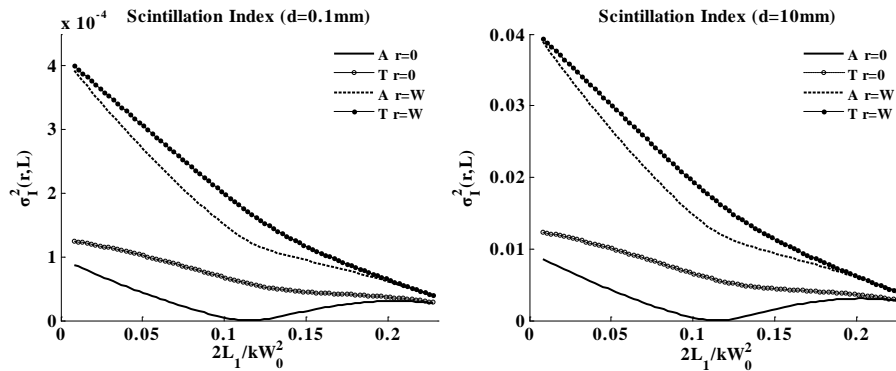


Fig. 5. Comparison of scintillation index with different thickness (T: thin phase screen; A: arbitrary thickness phase screen)

the thickness of phase screens when they are located in the same position. The results predicted by scintillation index model, Eq. (56), are according with those shown by DOC model, Eq. (47), because the weakening of coherence results in the fluctuation of irradiance as shown in Fig. 4 and Fig. 5.

6. Summary

In this paper, we, based on Rytov method and Andrews et al's [4–7] works, establish the mathematic models of statistical quantities for Gaussian beam propagation through an arbitrary thickness phase screen and developed the analytical results. The comparison between Andrews' thin phase screen approximation results and our results shows that Andrews' results are concise but has its own limitation, and our results are suitable for more generalized case, though complicate, especially for the scintillation index. For mean irradiance on receiver plane and the MCF of thin phase screen ($d/L < 0.01$), the two models have few differences, so both of them can be used to describe these quantities accurately. But for MCF of thick phase screen, DOC, and scintillation index, we'd better to utilize the arbitrary thickness phase screen model to describe them, because the thin phase screen model has intrinsic error due to the approximation. The paper offers a theory fundamental, for AO and laser communication application research in laboratory.

Acknowledgments

The authors are very thankful to the reviewers for valuable comments. This work was supported by the Innovation Foundation of the Chinese Academy of Sciences III under grant O98Y32C100.